Control of spiral waves in optogenetically modified cardiac tissue by periodic optical stimulation

Qi-Hao Li,[1,2] Yuan-Xun Xia,[1] Shu-Xiao Xu,[1] Zhen Song,[2] Jun-Ting Pan,[3] Alexander V. Panfilov,[4,5,6,*] and Hong Zhang[1,†]

[1]*Zhejiang Institute of Modern Physics and Department of Physics, Zhejiang University, Hangzhou 310027, China*

[2]*Department of Mathematics and Theories, Peng Cheng Laboratory, Shenzhen 518066, China*

[3]*Ocean College, Zhejiang University, Zhoushan 316021, China*

[4]*Department of Physics and Astronomy, Ghent University, Ghent 9000, Belgium*

[5]*Laboratory of Computational Biology and Medicine, Ural Federal University, Ekaterinburg 620002, Russia*

[6]*World-Class Research Center "Digital biodesign and personalized healthcare," Sechenov University, Moscow 119146, Russia*

(Received 7 December 2021; accepted 30 March 2022; published 21 April 2022)

Resonant drift of nonlinear spiral waves occurs in various types of excitable media under periodic stimulation. Recently a novel methodology of optogenetics has emerged, which allows to affect excitability of cardiac cells and tissues by optical stimuli. In this paper we study if resonant drift of spiral waves in the heart can be induced by a homogeneous weak periodic optical stimulation of cardiac tissue. We use a two-variable and a detailed model of cardiac tissue and add description of depolarizing and hyperpolarizing optogenetic ionic currents. We show that weak periodic optical stimulation at a frequency equal to the natural rotation frequency of the spiral wave induces resonant drift for both depolarizing and hyperpolarizing optogenetic currents. We quantify these effects and study how the speed of the drift and its direction depend on the initial conditions. We also derive analytical formulas based on the response function theory which correctly predict the drift velocity and its trajectory. We conclude that optogenetic methodology can be used for control of spiral waves in cardiac tissue and discuss its possible applications.

DOI: 10.1103/PhysRevE.105.044210

I. INTRODUCTION

Spiral waves represent a typical example of self-organized processes in spatially extended nonequilibrium systems with quite different nature starting from physics to chemistry and biology [1–3]. Examples include the Belousov-Zhabotinsky (BZ) reaction [4,5], CO oxidation on platinum [6], heart muscle [7,8], retina of eyes [9], aggregations of Dictyostelium discoideum amoebae [10], and frog eggs, through which calcium waves propagate [11].

The attractiveness of investigating the dynamics of spiral waves is not only because they have a special structure, i.e., the spiral tip which is regarded as a topological defect [12,13], but more importantly they contribute to an underlying class of cardiac diseases, such as tachycardia and fibrillation [14–16]. Thus, it is important to know how to control spiral waves so that we can prevent or suppress them.

Optogenetics has emerged as an alternative method for electrical control of the heart, where optical stimuli are used to elicit a bioelectric response in tissue modified to express photosensitive proteins (opsins) [17,18]. Its capabilities have been extensively used to study the mechanisms underlying the incidence, maintenance, and control of cardiac arrhythmias [19–22].

Recently, the control of spiral waves in optogenetically modified cardiac tissue by using optical stimuli has attracted much attention [23–25]. Burton *et al.* [23] studied the optical control of spiral waves in cardiac tissue and demonstrated the light-controlled reversal of the cardiac spiral wave chirality. Majumder *et al.* [24] showed that the light-guided manipulation of the core of spiral waves can be used to establish the real-time spatiotemporal control over the position, number, and rotation of these spirals in cardiac tissue. Both these studies demonstrate the manipulation of spiral waves by suprathreshold optical stimulation, which has the ability to initiate new waves in cardiac tissue. In Ref. [25], Hussaini *et al.* studied the dynamics of spiral waves in optogenetically modified cardiac tissue at subthreshold optical stimulation and showed that spiral waves undergo a drift in the presence of a gradient of optical stimulation.

In this paper, we revisit in view of optogenetics one of the most studied methodologies for control of spiral waves in excitable medium: resonance drift. Resonance drift was initially found theoretically and in BZ reaction. It was shown that periodic variations of properties of excitable medium in time results in drift of the spiral [26–34] and the most pronounced displacement occurred when the period of variations was equal to the period of the spiral wave.

In this paper we study manifestation of resonance drift in optogenetically modified cardiac tissue by applying homogeneous weak periodic (i.e., subthreshold) optical stimulation at a frequency equal to the natural rotation frequency of the spiral wave. We numerically show that both depolarizing and hyperpolarizing optogenetic currents induce drift of spirals under weak periodic stimulation and study its properties in various conditions. We also develop a analytical

*Corresponding author: Alexander.Panfilov@UGent.be

†Corresponding author: hongzhang@zju.edu.cn

description of this process by applying the response function theory and compare its predictions with numerical simulations. We show that optogenetic methodology for both depolarizing and hyperpolarizing ion currents can be successfully used for control of spiral waves in cardiac tissue and no feedback loops are needed for control of the system.

II. MODELS AND METHODS

A. Two-state variable model

To describe the electrical activities of cardiac tissue, we use the general Barkley model [35,36]:

$$\frac{\partial u}{\partial \mathrm{t}} = \frac{1}{\varepsilon}u(1-u)\left(u - \frac{v+b}{a}\right) + D\nabla^2 u + I_{\mathrm{optp}}, \quad (1a)$$

$$\frac{\partial v}{\partial \mathrm{t}} = u - v, \quad (1b)$$

where u is the fast (voltage) variable while v is the slow (gating) variable; ε, a, and b are model parameters; D is the diffusion coefficient. ε, a, b, and D are fixed at 0.02, 0.9, 0.08, and 1.0, respectively; when we choose such parameter configurations, the spiral undergoes rigid rotation. In simulations, Eq. (1) is integrated on a 500×500 grid via Euler method with no-flux boundary conditions. The space step and the time step are fixed at $\Delta x = \Delta y = 0.15$ and $\Delta t = 0.001\,25$, respectively.

In this paper, we consider the optical-induced current I_{optp} in cardiac tissue [37]. Depending on which opsins being expressed the optical-induced current I_{optp} can be divided into the depolarizing current and the hyperpolarizing current [38,39]. In model (1) a depolarized state corresponds to $u = u_{\max} = 1$; thus, we use $u = 1$ as a Nernst potential for the depolarizing current correspondingly. Also, we assume that the conductance of the optogenetic channels is g which depends on the light intensity I_1 at given time t. For simplicity, we set $g = I_1$; thus, we get the following representation: $I_{\mathrm{optp}} = -g(u-1) = -I_1(u-1)$. Similarly, we can use $I_{\mathrm{optp}} = -g(u-0) = -I_1(u-0)$ to simulate the optical-induced hyperpolarizing current since $u = u_{\min} = 0$ corresponds to the resting potential of model (1). We add homogeneous periodic optical stimulation in the form of $I_1 = I_0[1 + \cos(\omega_I t + \phi_I)] \geqslant 0$ to study the effect of weak periodic optical stimulation on spiral waves. ω_I is the angular frequency and ϕ_I is the initial phase. Under weak optical stimulation $I_0 \ll 1$, no new electric waves emerge, and electric signals can still conduct in optical-stimulated regions [25].

B. Ionic model

Detailed mathematical models of the ionic currents in cardiac tissue have been developed to provide a better understanding of the electrical activity in the heart. To describe the electric activity of cardiac tissue, we also consider the Luo-Rudy model that is based on ventricular cardiomyocytes [40]:

$$\frac{\partial V}{\partial t} = -\frac{I_{\mathrm{ion}} + I_{\mathrm{optp}}}{C_m} + \nabla\cdot(D\nabla V), \quad (2a)$$

$$I_{\mathrm{ion}} = I_{Na} + I_{si} + I_K + I_{K1} + I_{Kp} + I_b, \quad (2b)$$

where V is the transmembrane voltage, and I_{ion} is the total ionic currents which consist of a fast sodium current I_{Na}, a slow inward current I_{si}, a time-dependent potassium current I_K, a time-independent potassium current I_{K1}, a plateau potassium current I_{Kp}, and a time-independent background current I_b. $C_m = 1\ \mu\mathrm{F/cm^2}$ is the membrane capacitance, and $D = 0.001\ \mathrm{cm^2/ms}$ is the current diffusion coefficient. In simulations, we take $G_{si} = 0$, $G_{Na} = 5$, $G_k = 0.423$ and keep $j \equiv 1$, which may generate a rigidly rotating spiral wave [41,42].

To include light sensitivity, the model (2) is coupled to a mathematical model of a light-activated protein called channelrhodopsin-2 (ChR2). This protein is a light-gated cation channel that responses to blue light. The ChR2 depolarizing current I_{optp} caused by optical stimulation I_1 is described by the following equation [43]:

$$\begin{aligned}
I_{\mathrm{optp}} &= g_{\mathrm{ChR2}}G(V)(O_1 + \gamma O_2)(V - E_{\mathrm{ChR2}}),\\
O_1 + O_2 + C_1 + C_2 &= 1,\\
G(V) &= [10.6408 - 14.6408\exp(-V/42.7671)]/V,\\
dC_1/dt &= G_r C_2 + G_{d1}O_1 - k_1 C_1,\\
dO_1/dt &= k_1 C_1 - (G_{d1} + e_{12})O_1 + e_{21}O_2,\\
dC_2/dt &= G_{d2}O_2 - (k_2 + G_r)C_2,\\
dO_2/dt &= k_2 C_2 - (G_{d2} + e_{21})O_2 + e_{12}O_1,
\end{aligned} \quad (3)$$

where g_{ChR2} is the maximal channel conductance, $G(V)$ is the voltage rectification function, O_1 and O_2 are the open-state probabilities of the ChR2, $\gamma = 0.1$ is the ratio of conductance of open states (O_2/O_1), and E_{ChR2} is the reversal potential of the channel. e_{12}, e_{21}, k_1, k_2, G_{d1}, G_{d2}, and G_r are kinetic parameters representing the transition of ChR2 with the state O_1, O_2, C_1, and C_2. Their equations are

$$\begin{aligned}
e_{12} &= 0.011 + 0.005\ln(1 + I_1/0.024),\\
e_{21} &= 0.008 + 0.004\ln(1 + I_1/0.024),\\
k_1 &= \varepsilon_1 F p,\ k_2 = \varepsilon_2 F p,\\
F &= \sigma_{\mathrm{ret}} I_1 \lambda/(w_{\mathrm{loss}} hc),\\
dp/dt &= [S_0(\theta) - p]/\tau_{\mathrm{ChR2}},\\
S_0(\theta) &= 0.5(1 + \tanh(120(\theta - 0.1))),\\
G_{d1} &= 0.075 + 0.043\tanh[(V + 20)/(-20)],\\
G_{d2} &= 0.05,\ \theta = 100 I_1,\\
G_r &= 4.345\ 87\times 10^{-5}\exp(-0.021\ 153\ 927\ 4V),
\end{aligned}$$

and furthermore, $\sigma_{\mathrm{ret}} = 12\times 10^{-20}\ \mathrm{m^2}$, $w_{\mathrm{loss}} = 0.77$, $\tau_{\mathrm{ChR2}} = 1.3\ \mathrm{ms}$, $\lambda = 470\ \mathrm{nm}$ and $hc = 1.986\,446\times 10^{-25}\ \mathrm{kg\ m^3/s^2}$. Table 1 in Ref. [43] shows more specific definitions of these parameters.

By substituting Eq. (3) into Eq. (2), we can stimulate the system optically at the 2D monodomain level. Equations (2) and (3) are integrated on 400×400 grids via the Euler method with no-flux boundary conditions. The space step and the time step are fixed at $\Delta x = \Delta y = 0.015$ cm and $\Delta t = 0.005$ ms, respectively.

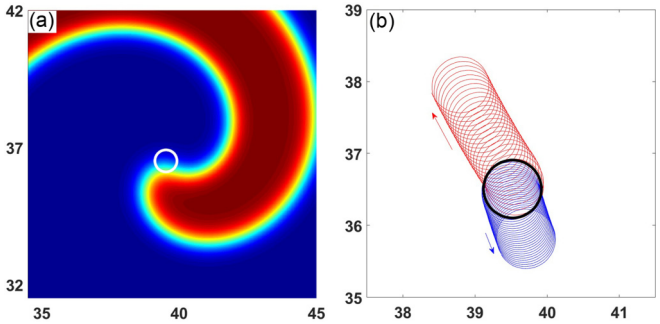

FIG. 1. Effects of weak periodic optical stimulation on the spiral wave dynamics in the Barkley model. (a) Spiral wave before stimulation. The wave rotates clockwise around a circular core, i.e., the path of the spiral tip (white). The model parameters are $\varepsilon = 0.02$, $a = 0.9$, and $b = 0.08$. (b) Spiral wave dynamics under a homogeneous periodic optical stimulation at a frequency equal to the natural rotation frequency of the spiral wave. Red line: under application of the depolarizing current. Blue line: under application of the hyperpolarizing current. In both cases the spiral wave tip trajectory is a loopy line with straight net translation. Simulations for optical stimulation $I_1 = I_0[1 + \cos(\omega_I t + \phi_I)]$ with $I_0 = 0.005$, $\omega_I = \omega_0$, and $\phi_I = 0$. The spiral tip is determined as the intersection of the isolines of $u = 0.5$ and $v = a/2 - b$ [44].

III. NUMERICAL RESULTS

We begin with the Barkley model (1). In Fig. 1(a), we generate a clockwise rigidly rotating spiral wave with a rotation frequency $\omega_0 = 1.742$. Rigid rotation is the simplest regime of the spiral wave motion. Such rotation occurs with a constant angular velocity and the spiral tip describes a circular trajectory. The tip is the inner end of the spiral arm, and its location is defined as the intersection of the isolines of u and v.

We add homogeneous weak periodic optical stimulation to the system to study its effect on the spiral wave. Numerical simulations show that when ω_I and ω_0 are equal, the spiral wave undergoes a resonant drift. The drift trajectory of the tip is displayed in Fig. 1(b) under periodic optical stimulation with $I_0 = 0.005$, $\omega_I = \omega_0$, and $\phi_I = 0$. The red line and the blue line represent the spiral tip trajectory under the optical-induced depolarizing and hyperpolarizing currents, respectively. The spiral tip initially rotates around the central black circle. Due to periodic stimulation the tip of the spiral undergoes induced drift along the trajectory which consists of the rotation and the translation along a straight line.

Now we study the resonant drift of the spiral wave in more detail. The drift velocity of the spiral wave is related to I_0, ϕ_I and its initial phase Φ. By selecting appropriate ϕ_I or Φ, it is possible to choose any drift direction Θ.

We first fix I_0, ϕ_I and change Φ in the range of $0-2\pi$. In Fig. 2, the drift speed $|\dot{R}|$ and the drift direction Θ are plotted for different Φ. We can see that $|\dot{R}|$ is independent of Φ [Figs. 2(a) and 2(c)], and Θ changes linearly with Φ [Figs. 2(b) and 2(d)].

We also changed the initial phase of the stimulation ϕ_I in the range of $0-2\pi$ and found similar dependencies (see Supplemental Material, Fig. S1 [45]). The results presented in Figs. 2 and S1 confirm the rotational symmetry of the problem and show that the drift direction of spiral waves can be significantly affected by the initial phases of periodic optical stimulation and spiral wave. All the drift directions are also accessible by changing the initial phase of the periodic optical stimulation or spiral wave.

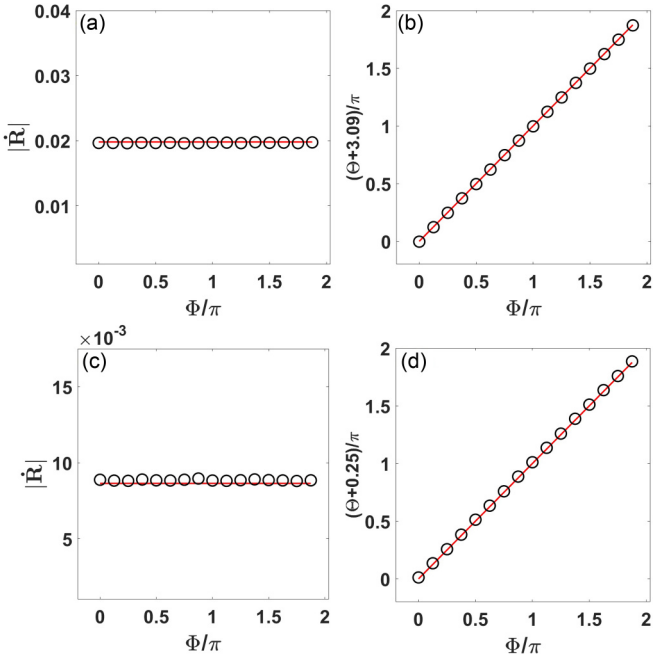

FIG. 2. The relationship between the drift velocity and the initial phase Φ of the spiral wave with $I_0 = 0.005$, $\omega_I = \omega_0$, and $\phi_I = 0$. (a), (c) Drift speed $|\dot{R}|$ vs Φ. (b), (d) Drift direction Θ vs Φ. The white circle and the red line represent numerical results and theoretical results, respectively. Top row: the depolarizing current case. Bottom row: the hyperpolarizing current case.

Thus far, we have shown, through direct numerical simulations of the Barkley model, that under weak periodic optical stimulation with $\omega_I = \omega_0$ the drift speed $|\dot{R}|$ of the spiral is independent of Φ and ϕ_I, and the drift direction Θ depends both on Φ and ϕ_I.

The Barkley model used in this paper is a generic model for excitable medium. Although it reproduces main properties of propagating waves in cardiac tissue it does not represent in detail the process of generation of cardiac action potential, which may have influence on the resonant drift of spiral waves in cardiac tissue. Therefore, we further investigated the drift behavior of spiral waves under periodic optical stimulation in the Luo-Rudy model (2) which is a detailed mathematical model for cardiac tissue and includes description of the main ionic currents generating cardiac action potential.

Figure 3(a) shows a rigidly rotating spiral wave in the Luo-Rudy model. We study the effects of weak periodic optical stimulation on the spiral wave by adding a weak periodic optical stimulation in the form of $I_1 = I_0[1 + \cos(\omega_I t + \phi_I)]$. Similar to the Barkley model, the spiral wave undergoes a resonant drift [Fig. 3(b)]. The drift is also along the loopy trajectory which consists of the rotation and the linear translation as displayed in Fig. 3(b). Additional simulations confirmed that, same as the Barkley model, the drift direction Θ of the spiral also changes linearly with Φ or ϕ_I (The relationship of drift direction Θ and Φ or ϕ_I is not shown in the figures).

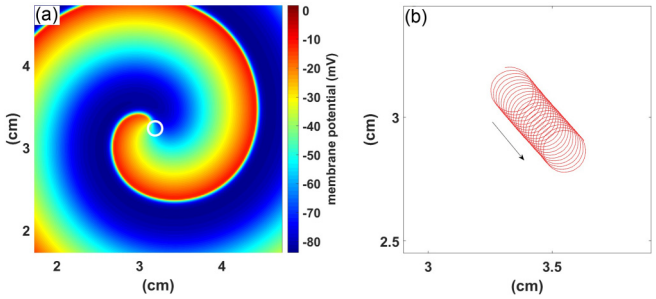

FIG. 3. Effects of weak periodic optical stimulation on the spiral wave dynamics in the Luo-Rudy model with $\overline{G}_{Na} = 5$, $\overline{G}_K = 0.423$, $\overline{G}_{Si} = 0.0$, and $j \equiv 1$. (a) Clockwise rigidly rotating spiral wave. The path of the spiral tip (white) is a circle. (b) Spiral wave dynamics under homogeneous periodic optical stimulation: $I_1 = I_0[1 + \cos(\omega_I t + \phi_I)]$ with $I_0 = 0.001$ mW/mm^2, $\omega_I = \omega_0 = 0.1403$ rad/ms, and $\phi_I = 0$. The tip trajectory exhibits a loopy line with straight net translation (red). The spiral tip is determined by the intersection point of two contour lines of the voltage corresponding to -35 mV with the time interval of 2 ms [41].

IV. THEORETICAL ANALYSIS

To analyze theoretically the drift behavior of spiral waves in cardiac tissue under the influence of homogeneous weak periodic optical stimulation, we rewrite the Barkley model in the matrix form:

$$\partial_t \mathbf{u} = \mathbf{F}(\mathbf{u}) + \mathbf{D}\Delta\mathbf{u} + \mathbf{h}, \tag{4}$$

where $\mathbf{u} = [u, v]^T$, $\mathbf{F}(\mathbf{u}) = [\varepsilon^{-1}u(1-u)[u-(v+b)/a], u-v]^T$, $\mathbf{D} = \mathrm{diag}(1, 0)$. $\mathbf{h}$ represents the optical stimulation. If $\mathbf{h} = -I_0[1 + \cos(\omega_I t + \phi_I)](u-1)[1, 0]^T$, the optical stimulation generates the depolarizing current, and when $\mathbf{h} = -I_0[1 + \cos(\omega_I t + \phi_I)](u-0)[1, 0]^T$, the optical stimulation generates the hyperpolarizing current.

In the absence of optical stimulation, a rigidly clockwise-rotating spiral wave solution to Eq. (4) has the form

$$\mathbf{U}(\vec{r}, t) = \mathbf{U}(\rho(\vec{r} - \vec{R}), \vartheta(\vec{r} - \vec{R}) + \omega_0 t - \Phi), \tag{5}$$

where $\vec{R} = (X, Y)^T$ is the rotation center of spiral waves; $\rho(\vec{r} - \vec{R})$ and $\vartheta(\vec{r} - \vec{R})$ are polar coordinates constructed with $\vec{R}$ as the center. We set $\vec{\zeta}_{\mathrm{tip}}(t)$ as the tip of the spiral wave. The initial phase Φ is the angle between $\vec{\zeta}_{\mathrm{tip}}(t = 0) - \vec{R}$ and x axis, which is measured counterclockwise from the positive x axis.

According to the response function theory [46–48], for a rigidly rotating spiral wave, the drift velocity can be analyzed in a reference polar coordinate system corotating with the initial phase and the angular frequency of the spiral wave around its rotation center. In the reference system, $\vec{R}' = 0$ and $\Phi' = 0$. Following the methods in Ref. [49], we can obtain the drift velocity of spiral waves under weak optical stimulation with $\omega_I = \omega_0$:

$$\dot{R}(t) = e^{i\Phi}\int_{t-\pi/\omega_0}^{t+\pi/\omega_0} \frac{\omega_0 d\tau}{2\pi} e^{-i\omega_0\tau}\left\langle \mathbf{W}^{(1)}(\Phi' = 0), -I_0[1 + \cos(\omega_0\tau + \phi_I)][U(\Phi' = 0) - 1]\begin{pmatrix}1\\0\end{pmatrix}\right\rangle, \tag{6a}$$

$$\dot{R}(t) = e^{i\Phi}\int_{t-\pi/\omega_0}^{t+\pi/\omega_0} \frac{\omega_0 d\tau}{2\pi} e^{-i\omega_0\tau}\left\langle \mathbf{W}^{(1)}(\Phi' = 0), -I_0[1 + \cos(\omega_0\tau + \phi_I)][U(\Phi' = 0) - 0]\begin{pmatrix}1\\0\end{pmatrix}\right\rangle, \tag{6b}$$

where $\mathbf{W}^{(1)}$ is one of the response functions of the spiral wave with critical eigenvalue $-i\omega_0$. Equation (6a) represents the depolarizing current and Eq. (6b) represents the hyperpolarizing current. The time-independent term in the inner product $\langle \mathbf{w}, \mathbf{v} \rangle$ is always equal to zero after integration of one period time. Therefore, the drift velocity can be expressed as

$$\dot{R} = \frac{I_0\mu}{2} e^{i(\Phi + \phi_I + \nu)}, \tag{7}$$

where

$$\mu e^{i\nu} = \left\langle \mathbf{W}^{(1)}(\rho, \theta, \Phi' = 0), \begin{matrix}1 - U(\Phi' = 0)\\0\end{matrix}\right\rangle, \tag{8a}$$

$$\mu e^{i\nu} = \left\langle \mathbf{W}^{(1)}(\rho, \theta, \Phi' = 0), \begin{matrix}0 - U(\Phi' = 0)\\0\end{matrix}\right\rangle. \tag{8b}$$

$R(t) = X + iY$ is the complex coordinate constructed with the instantaneous rotation center location of the spiral wave. Equation (8a) represents the depolarizing current and Eq. (8b) represents the hyperpolarizing current. Therefore, $\dot{R} = |\dot{R}|e^{i\Theta}$ is the drift velocity, $|\dot{R}|$ is the drift speed, and Θ is the drift direction. From Eq. (7), we obtain finally

$$|\dot{R}| = \frac{I_0\mu}{2}, \quad \Theta = \Phi + \phi_I + \nu. \tag{9}$$

Using the open-source software DXSPIRAL [50], we can compute the drift coefficients μ and ν. For the parameters in Fig. 1, we get $\mu = 7.9218$ and $\nu = -3.0862$ for the depolarizing current and $\mu = 3.4542$ and $\nu = -0.2538$ for the hyperpolarizing current, respectively.

Based on Eq. (9), we can find the following characteristics of the resonant drift of spiral waves in cardiac tissue induced by periodic optical stimulation. First, the drift speed $|\dot{R}|$ is directly proportional to the amplitude of the periodic optical stimulation I_0, but independent of the initial phase Φ of the spiral wave and the initial phase ϕ_I of the periodic optical stimulation. It agrees well with the numerical results displayed in Figs. 2(a), 2(c), and S1(a), S1(c). Furthermore, the values of the drift speed $|\dot{R}|$ predicted by the theory [the red solid lines in Figs. 2(a), 2(c), and S1(a), S1(c)] are quantitatively consistent with those measured directly from the numerical simulations. Second, the drift direction Θ changes linearly with Φ, i.e., $\Delta\Theta = \Delta\Phi$ when ϕ_I is fixed. They are quantitatively consistent with the numerical results as shown in Figs. 2(b) and 2(d). Third, the spiral wave drifts along different directions when we change ϕ_I, i.e., $\Delta\Theta = \Delta\phi_I$ when Φ is fixed. They also quantitatively agree with the numerical results as shown in Figs. S1(b) and S1(d).

Now let us study the trajectory of a spiral tip in more detail. We substantially extended the size of the domain

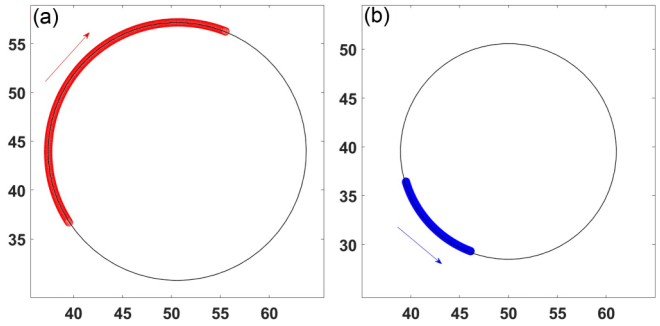

FIG. 4. The same as in Fig. 1(b) but in a large domain and extended running time. The tip trajectory exhibits a loopy line (red and blue) and the drift trajectory of the spiral rotation center is a circle. The black line is the fitted curve for the drift trajectory of the spiral rotation center. (a) The depolarizing current case, where the radius is $r = 13.2083$. (b) The hyperpolarizing current case, where the radius is $r = 11.0472$. The periodic optical stimulation $I_1 = I_0[1 + \cos(\omega_I t + \phi_I)]$ with amplitude of $I_0 = 0.005$.

and studied the drift trajectory under weak periodic optical stimulation $\mathbf{h} = -I_0[1 + \cos(\omega_I t + \phi_I)](u-1)[1, 0]^T$ for depolarizing and $\mathbf{h} = -I_0[1 + \cos(\omega_I t + \phi_I)](u-0)[1, 0]^T$ for hyperpolarizing current. The result is shown in Figs. 4(a) and 4(b). We see that actually spiral drift trajectory here is a circle of a large radius.

In Ref. [48], Biktasheva *et al.* pointed out that spiral waves will undergo resonant drift under general weak periodic force $\mathbf{h} = I_0 \cos(\omega_0 t + \phi_I)[1, 0]^T$ ($I_0 \ll 1$) and the typical trajectory of a resonantly drifting spiral wave is a large circle of radius $r = O(I_0^{-1}) \gg 1$. Therefore, under weak periodic force $\mathbf{h} = I_0 \cos(\omega_0 t + \phi_I)[1, 0]^T$, the spiral drift trajectory is close to a straight line in a limited size system.

Note, however, that in our case, since the light intensity is no less than zero, the expression for the periodic force has a different form: instead of $I_0 \cos(\omega_0 t + \phi_I)[1, 0]^T$ the periodic force is $-I_0[1 + \cos(\omega_0 t + \phi_I)](u-1)[1, 0]^T$ or $-I_0[1 + \cos(\omega_0 t + \phi_I)](u-0)[1, 0]^T$.

As a result, in our case the drift along the circle of finite radius is due to a different effect: change of frequency of spiral wave. Because of that, such circular drift will also occur in an finite system as $r \approx O(1)$. Let us show it theoretically.

For weak optical stimulation with $\omega_I = \omega_0$, we can obtain that the change of the frequency is

$$\dot{\Phi}(t) = \int_{t-\pi/\omega_0}^{t+\pi/\omega_0} \frac{\omega_0 d\tau}{2\pi} \left\langle \mathbf{W}^{(0)}(\Phi' = 0), -I_0[1 + \cos(\omega_0 \tau + \phi_I)][U(\Phi' = 0) - 1] \begin{pmatrix} 1 \\ 0 \end{pmatrix} \right\rangle, \tag{10a}$$

$$\dot{\Phi}(t) = \int_{t-\pi/\omega_0}^{t+\pi/\omega_0} \frac{\omega_0 d\tau}{2\pi} \left\langle \mathbf{W}^{(0)}(\Phi' = 0), -I_0[1 + \cos(\omega_0 \tau + \phi_I)][U(\Phi' = 0) - 0] \begin{pmatrix} 1 \\ 0 \end{pmatrix} \right\rangle, \tag{10b}$$

Eq. (10a) for the depolarizing current and Eq. (10b) for the hyperpolarizing current. After integration, one can get

$$\dot{\Phi} = I_0 \chi, \tag{11}$$

where

$$\chi = \left\langle \mathbf{W}^{(0)}(\Phi' = 0), \begin{matrix} 1 - U(\Phi' = 0) \\ 0 \end{matrix} \right\rangle \quad \text{or } \chi = \left\langle \mathbf{W}^{(0)}(\Phi' = 0), \begin{matrix} 0 - U(\Phi' = 0) \\ 0 \end{matrix} \right\rangle.$$

$\mathbf{W}^{(0)}$ is one of the response functions of the spiral wave with critical eigenvalue 0. For the parameters in Fig. 1, we get $\chi = -0.3612$ for the depolarizing current and $\chi = 0.1427$ for the hyperpolarizing current, respectively.

From Eq. (9), we can know that $\dot{\Theta} = \dot{\Phi}$, and that the drift speed $|\dot{R}|$ is independent of Φ; thus, we know that $\dot{\Phi}$ is the angular velocity of the resonant drift and the radius of the circle is

$$r = |\dot{R}|/|\dot{\Phi}| = \left| \frac{\mu}{2\chi} \right| = O(1). \tag{12}$$

Thus, we see that compared to the results of Ref. [48], the radius in our case is indeed $r \approx O(1)$ and does not depend on I_0. In Fig. 4, we extend the running time of Fig. 1(b) and observe that the spiral wave drifts along a circle of radius $r = 13.2083$ for the depolarizing current and $r = 11.0472$ for the hyperpolarizing current. All are close to the radius $r = 10.9669$ for the depolarizing current and $r = 12.1064$ for the hyperpolarizing current, which are predicted by Eq. (12). If we decrease I_0 to 0.001, the observed radius r in numerical simulations becomes $r = 11.8683$ for the depolarizing current and $r = 11.7000$ for the hyperpolarizing current, which are closer to the radius that the theory predicts.

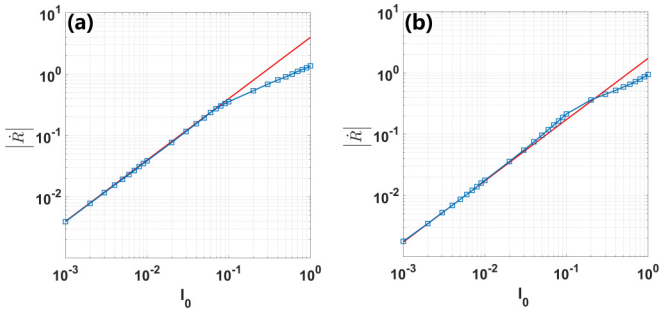

FIG. 5. The relationship between the drift speed $|\dot{R}(t)|$ and I_0. The red line indicates the theoretical results and the blue square line represents the numerical results. (a) The depolarizing current case. (b) The hyperpolarizing current case.

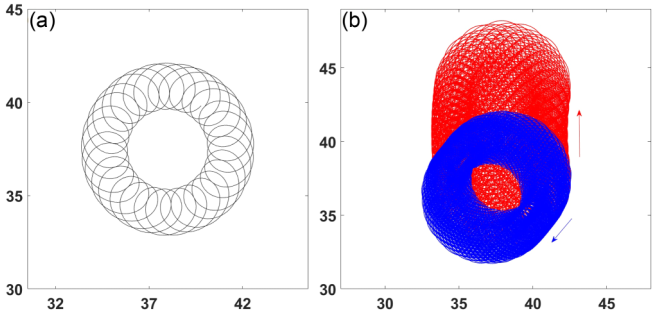

FIG. 6. Resonant drift of the meandering spiral wave. (a) Meandering trajectory of the spiral tip. (b) The spiral tip trajectory exhibits straight net translation. Red line: the depolarizing current case. Blue line: the hyperpolarizing current case.

V. DISCUSSION

A. Effect of the amplitude

Through the previous content, we have observed the resonant drift of the rigidly rotating spiral wave under weak periodic optical stimulation and analyzed it theoretically. In Fig. 5, we study the relationship between the drift speed $|\dot{R}(t)|$ of spiral waves and the amplitude of periodic optical stimulation I_0 in a wide range of the amplitude. We see that when I_0 is relatively small, the theoretical results of the drift speed agree well with its numerical results. However, when I_0 increases, the simulation results start to deviate from the theoretical results.

B. Cardiac parameters

In our paper we used a generic Barkley model for cardiac tissue and also an ionic Luo-Rudy model. A typical drift speed of a spiral wave in Luo-Rudy model was 0.347 cm/s for $I_0 = 0.001\,\mathrm{mW/mm^2}$. Note, however, that in a modification of Luo-Rudy model used in our paper a typical period of spiral wave is 44.8 ms and a spatial wavelength of a spiral is 1.54 cm. This means that in dimensionless units, when a spatial variable is expressed in wavelength λ_s and time is normalized by a period of rotation T_s, the drift speed will be $0.0101\,\lambda_s/\mathrm{T}_s$ with $I_0 = 0.001\,\mathrm{mW/mm^2}$, or during one stimulation cycle, a spiral wave core shifts $0.0101\,\lambda_s$. As a typical wavelength of a rotor is of the order of 3−7 cm and a period of an arrhythmia in the human heart is on the order of 150−200 ms [51,52], we can expect that for parameters used in our simulations a typical drift speed in the human heart will be 0.151–0.469 cm/s. As the typical size of ventricles in the human heart is on the order of 10 cm, we estimate that bringing spiral waves from the center to the outer edge of the heart will take the order of 10−30 s, which in our view, is relevant for clinical interventions. The amplitude of the stimulation is realistic, as it is based on a realistic model of optogenetic channel. In a generic Barkley model similar estimates give $0.00635\,\lambda_s/\mathrm{T}_s$ for the depolarizing current and $0.00288\,\lambda_s/\mathrm{T}_s$ for the hyperpolarizing current with $I_0 = 0.005$. The expected drift speed of arrhythmias will be 0.0953−0.296 cm/s for the depolarizing current and 0.0433−0.135 cm/s for the hyperpolarizing current. According to Fig. 5, with I_0 increasing to 0.1, Barkley model estimates give $0.109\,\lambda_s/\mathrm{T}_s$ for the depolarizing current and $0.0747\,\lambda_s/\mathrm{T}_s$ for the hyperpolarizing current. The expected drift speed of arrhythmias will be 1.64–5.09 cm/s for the depolarizing current and 1.12 − 3.45 cm/s for the hyperpolarizing current. Thus, it takes about 1−4 s to move a spiral wave from the center to the outer edge of the heart.

C. Resonant drift for meandering spirals

The spiral wave dynamics was also extensively studied in the chemical excitable medium: the BZ reaction. Also, the resonant drift phenomenon for spiral waves subjected to the external periodic forcing has been studied in numerous experiments as well as numerical simulations in light-sensitive BZ reactions [28–34]. And, in light-sensitive BZ reactions, the resonant drift has been observed for both rigidly rotating spiral waves and meandering spiral waves.

Considering that rigid rotation is not the only possible regime of spiral waves in cardiac tissue, we further applied weak periodic stimulation to meandering spiral waves and also observed the resonant drift which is similar to that of the rigidly rotating spiral wave. The meandering spiral wave is generated by the general Barkley model [35,36] with ε, a, b, and D being 0.02, 0.58, 0.05, and 1.0, respectively. The meandering trajectory of the spiral tip is shown in Fig. 6(a). The drift trajectory of the spiral tip is shown in Fig. 6(b) under periodic optical stimulation with $I_0 = 0.001$ and $\omega_I = \omega_0 = 1.340$. ω_0 is the frequency of the meandering spiral wave, which corresponds to the primary simple rotation of the spiral tip [53,54]. Similar to a rigid rotation, we see a combination of the basic dynamics (in this case meandering) and a net linear shift of the trajectory.

D. Interaction with the boundary

In this paper we studied the process of resonant drift of spiral waves. This drift can bring spiral waves to the boundary of the medium and result in its elimination. However, we did not study in detail the process of interaction of spiral wave with the boundary. Note that interaction of a spiral wave with a no-flux boundary causes the drift of a spiral wave if its core is located sufficiently close to the boundary [55]. In addition to that, resonant drift can cause reflection of spiral waves from the boundary [46,56]. This resonant reflection is a complex

process and its control, e.g., by using the methods considered in Ref. [57], can make the annihilation of spiral wave at the boundary more efficiently. It would be interesting to study the interaction of resonant drift under periodic optical stimulation, considered in our paper, with the boundaries of the medium.

E. Resonance phenomenon in 3D

In this paper we studied resonance phenomenon in a 2D model for cardiac tissue. Compared to 2D, resonance phenomenon in 3D is largely underinvestigated. Also, because in 2D light can be applied to the surface of the tissue only, it would be interesting to find out effects of optical stimulation in that case as well. Here, one can use anatomical models of the heart as, e.g., in Refs. [58,59]. Note that in 3D there is also its own drift of 3D spiral wave [60,61], which can additionally contribute to the drift induced by the optical forcing.

F. Feedback control

In our cases the frequency of external forcing is constant and equals to the rotation frequency of the unperturbed spiral wave. In studies of resonant drift also other ways of frequency control were considered, and one of the most studied is the feedback control. In that case, the frequency of a perturbation was determined by an excitation frequency measured during the process of resonant drift. One of the most straightforward ways to do this is to measure the frequency by an electrode placed at some points in the tissue. In that case instead of motion along a straight line the spiral wave tip approaches an asymptotic trajectory with a symmetry center located at the measuring point [62]. The trajectory depends on various conditions. They are locations of the measuring electrodes with respect to the location of a spiral wave core, the delay of stimulation after passage of the wave, and some other factors. As a result, the spiral wave core can approach that measuring point (attraction), or approach another attractor at some distance from the measuring point [62]. Another type of feedback control was considered in Ref. [63], where instead of local measurement of the period, a feedback signal was generated from the integration of state variables in a certain domain. In that case the drift velocity field of spiral core can be very complex and depends on the size and the shape of the integration domain. In Ref. [64] a feedback control based on simulated electrocardiograms was considered and it resulted in effective elimination of spiral waves in the tissue. It would be interesting to study how these and other ways of local and global feedback control work for subthreshold optical stimulation considered in our paper.

VI. CONCLUSION

In summary, we have numerically studied the drift of spiral waves in cardiac tissue under the influence of homogeneous weak periodic optical stimulation in the Barkley model and the Luo-Rudy model. We find that spiral waves undergo a resonant drift under weak periodic optical stimulation at frequencies equal to those of the spirals. Using the response function theory, we derive a drift velocity of spiral waves in the Barkley model due to weak periodic optical stimulation and all the theoretical results agree with the numerical results quantitatively. In addition, in the limited size system, we find that the drift trajectory of the spiral wave is a circle under weak periodic optical stimulation. Further theoretical analysis based on the response function theory has been proposed and the observed radius of the drift trajectory in numerical simulations is close to the radius that the theory predicts. We expect that the resonant drift under homogeneous weak periodic optical stimulation at a frequency equal to the natural rotation frequency of the spiral wave is a common phenomenon. We hope that this phenomenon can be observed in cardiac experiments, and that this simple method of controlling cardiac arrhythmias could be implemented in clinical applications.

ACKNOWLEDGMENTS

We are thankful to I. V. Biktasheva and V. N. Biktashev for valuable comments. This work was supported by the National Natural Science Foundation of China under Grant No. 12075203, and Research at Sechenov University was financed by the Ministry of Science and Higher Education of the Russian Federation within the framework of state support for the creation and development of World-Class Research Centers "Digital biodesign and personalized healthcare" Grant No. 075-15-2020-926.

[1] M. C. Cross and P. C. Hohenberg, Rev. Mod. Phys. **65**, 851 (1993).
[2] A. T. Winfree, *The Geometry of Biological Time* (Springer, Berlin, 2000).
[3] K. Tsuji and S. C. Müller, *Spirals and Vortices* (Springer Nature, Cham, Switzerland, 2019).
[4] A. T. Winfree, Science **175**, 634 (1972).
[5] Q. Ouyang and J. M. Flesselles, Nature (London) **379**, 143 (1996).
[6] S. Jakubith, H. H. Rotermund, W. Engel, A. von Oertzen, and G. Ertl, Phys. Rev. Lett. **65**, 3013 (1990).
[7] R. A. Gray, A. M. Pertsov, and J. Jalife, Nature (London) **392**, 75 (1998).
[8] S. Luther, F. H. Fenton, B. G. Kornreich, A. Squires, P. Bittihn, D. Hornung, M. Zabel, J. Flanders, A. Gladuli, L. Campoy, E. M. Cherry, G. Luther, G. Hasenfuss, V. I. Krinsky, A. Pumir, R. F. Gilmour Jr., and E. Bodenschatz, Nature (London) **475**, 235 (2011).
[9] N. A. Gorelova and J. Bures, J. Neurobiol. **14**, 353 (1983).
[10] S. Sawai, P. A. Thomason, and E. C. Cox, Nature (London) **433**, 323 (2005).
[11] J. Lechleiter, S. Girard, E. Peralta, and D. Clapham, Science **252**, 123 (1991).
[12] J. Davidsen, L. Glass, and R. Kapral, Phys. Rev. E **70**, 056203 (2004).

[13] D. B. Pan, B. W. Li, J. T. Pan, Q. H. Li, and H. Zhang, New J. Phys. **22**, 103015 (2020).

[14] Z. Qu, G. Hu, A. Garfinkel, and J. N. Weiss, Phys. Rep. **543**, 61 (2014).

[15] S. Alonso, M. Bär, and B. Echebarria, Rep. Prog. Phys. **79**, 096601 (2016).

[16] S. Nattel, F. Xiong, and M. Aguilar, Nat. Rev. Cardiol. **14**, 509 (2017).

[17] K. Deisseroth, Nat. Methods **8**, 26 (2011).

[18] A. Gruber, O. Edri, and L. Gepstein, Europace **20**, 1910 (2018).

[19] T. Bruegmann, D. Malan, M. Hesse, T. Beiert, C. J. Fuegemann, B. K. Fleischmann, and P. Sasse, Nat. Methods **7**, 897 (2010).

[20] C. A. Nyns, A. Kip, C. I. Bart, J. J. Plomp, K. Zeppenfeld, M. J. Schalij, A. A. F. D. Vries, and D. A. Pijnappels, Eur. Heart J. **38**, 2132 (2017).

[21] C. Crocini, C. Ferrantini, F. S. Pavone, and L. Sacconi, Prog. Biophys. Mol. Biol. **130**, 132 (2017).

[22] R. A. Quiñonez Uribe, S. Luther, L. Diaz-Maue, and C. Richter, Front. Physiol. **9**, 1651 (2018).

[23] R. A. B. Burton, A. Klimas, C. M. Ambrosi, J. Tomek, A. Corbett, E. Entcheva, and G. Bub, Nat. Photon. **9**, 813 (2015).

[24] R. Majumder, I. Feola, A. S. Teplenin, A. A. De Vries, A. V. Panfilov, and D. A. Pijnappels, eLife **7**, e41076 (2018).

[25] S. Hussaini, V. Venkatesan, V. Biasci, J. M. R. Sepúlveda, R. A. Q. Uribe, L. Sacconi, G. Bub, C. Richter, V. Krinski, U. Parlitz, R. Majumder, and S. Luther, eLife **10**, e59954 (2021).

[26] V. A. Davydov, V. S. Zykov, A. S. Mikhailov, and P. K. Brazhnik, Radiofiz. **31**, 547 (1988).

[27] A. S. Mikhailov, V. A. Davydov, and V. S. Zykov, Physica D **70**, 1 (1994).

[28] K. I. Agladze, V. A. Davydov, and A. S. Mikhailov, Pis'ma Zh. Éksp. Teor. Fiz. **45**, 601 (1987) [JETP Lett. **45**, 767 (1987)].

[29] O. Steinbock, V. Zykov, and S. C. Müller, Nature (London) **366**, 322 (1993).

[30] V. S. Zykov, O. Steinbock, and S. C. Müller, Chaos **4**, 509 (1994).

[31] M. Braune, A. Schrader, and H. Engel, Chem. Phys. Lett. **222**, 358 (1994).

[32] A. Schrader, M. Braune, and H. Engel, Phys. Rev. E **52**, 98 (1995).

[33] V. S. Zykov, G. Bordiougov, H. Brandtstadter, I. Gerdes, and H. Engel, Phys. Rev. E **68**, 016214 (2003).

[34] S. Kantrasiri, P. Jirakanjana, and O.-U. Kheowan, Chem. Phys. Lett. **416**, 364 (2005).

[35] D. Barkley, Physica D **49**, 61 (1991).

[36] P. Bittihn, *Complex Structure and Dynamics of the Heart* (Springer International Publishing, Cham, Switzerland, 2015).

[37] K. Nikolic, N. Grossman, M. S. Grubb, J. Burrone, C. Toumazou, and P. Degenaar, Photochem. Photobiol. **85**, 400 (2008).

[38] P. M. Boyle, J. C. Williams, C. M. Ambrosi, E. Entcheva, and N. A. Trayanova, Nat. Commun. **4**, 2370 (2013).

[39] M. Funken, D. Malan, P. Sasse, and T. Bruegmann, Front. Physiol. **10**, 498 (2019).

[40] C. H. Luo and Y. Rudy, Circ. Res. **68**, 1501 (1991).

[41] Z. Qu, F. Xie, A. Garfinkel, and J. N. Weiss, Ann. Biomed. Eng. **28**, 755 (2000).

[42] S. Alonso and A. V. Panfilov, Phys. Rev. Lett. **100**, 218101 (2008).

[43] J. C. Williams, J. Xu, Z. Lu, A. Klimas, X. Chen, C. M. Ambrosi, I. S. Cohen, and E. Entcheva, PLoS Comput. Biol. **9**, e1003220 (2013).

[44] D. Barkley, M. Kness, and L. S. Tuckerman, Phys. Rev. A **42**, 2489 (1990).

[45] See Supplemental Material at http://link.aps.org/supplemental/10.1103/PhysRevE.105.044210 for the relationship between drift velocity and initial phase of stimulation (Fig. S1).

[46] V. Biktashev and A. Holden, Chaos Solitons Fractals **5**, 575 (1995).

[47] I. V. Biktasheva, D. Barkley, V. N. Biktashev, G. V. Bordyugov, and A. J. Foulkes, Phys. Rev. E **79**, 056702 (2009).

[48] I. V. Biktasheva, D. Barkley, V. N. Biktashev, and A. J. Foulkes, Phys. Rev. E **81**, 066202 (2010).

[49] T. C. Li, X. Gao, F. F. Zheng, D. B. Pan, B. Zheng, and H. Zhang, Sci. Rep. **7**, 8657 (2017).

[50] D. Barkley, V. N. Biktashev, I. V. Biktasheva, G. Bordyugov, and A. Foulkes, DXSPIRAL: A code for studying spiral waves on a disk, http://cgi.csc.liv.ac.uk/~ivb/SOFTware/DXSpiral.html (2010).

[51] S. M. Narayan, D. E. Krummen, and W.-J. Rappel, J. Cardiovasc. Electrophysiol. **23**, 447 (2012).

[52] D. E. Krummen, J. Hayase, D. J. Morris, J. Ho, M. R. Smetak, P. Clopton, W.-J. Rappel, and S. M. Narayan, J. Am. Coll. Cardiol. **63**, 2712 (2014).

[53] G. S. Skinner and H. L. Swinney, Physica D **48**, 1 (1991).

[54] J. Schlesner, V. Zykov, H. Engel, and E. Schöll, Phys. Rev. E **74**, 046215 (2006).

[55] E. A. Ermakova and A. M. Pertsov, Biofizika **31**, 855 (1986).

[56] V. N. Biktashev and A. V. Holden, Phys. Lett. A **181**, 216 (1993).

[57] V. N. Biktashev and A. V. Holden, J. Theor. Biol. **169**, 101 (1994).

[58] R. H. Keldermann, K. H. W. J. ten Tusscher, M. P. Nash, C. P. Bradley, R. Hren, P. Taggart, and A. V. Panfilov, Am. J. Physiol. **296**, H370 (2009).

[59] P. M. Boyle, T. V. Karathanos, and N. A. Trayanova, JACC Clin. Electrophysiol **4**, 155 (2018).

[60] A. V. Panfilov, A. N. Rudenko, and V. I. Krinsky, Biofizika **31**, 850 (1986).

[61] S. Alonso, F. Sagués, and A. S. Mikhailov, Science **299**, 1722 (2003).

[62] S. Grill, V. S. Zykov, and S. C. Müller, Phys. Rev. Lett. **75**, 3368 (1995).

[63] V. S. Zykov and H. Engel, Physica D **199**, 243 (2004).

[64] A. V. Panfilov, S. C. Müller, V. S. Zykov, and J. P. Keener, Phys. Rev. E **61**, 4644 (2000).